RSC Advances

PAPER

View Article Online
View Journal | View Issue

Cite this: *RSC Adv.*, 2021, **11**, 18787

Synergistic effect of copolymeric resin grafted 1,2-benzisothiazol-3(2*H*)-one and heterocyclic groups as a marine antifouling coating†

Miao Dong,[ab] Zheng Liu,[b] Yuxing Gao,[a] Xuemei Wang,[b] Junhua Chen[ab] and Jianxin Yang*[ab]

Received 8th March 2021
Accepted 13th May 2021

DOI: 10.1039/d1ra01826d

rsc.li/rsc-advances

In order to find a new type of antifouling coating with higher biological activity and more environmental protection, heterocyclic compounds and benzisothiazolinone were introduced into acrylic resin to prepare a new type of antifouling resin. In this study, a series of grafted acrylic resins simultaneously containing benzoisothiazolinone and heterocyclic monomers were prepared by the copolymerization of an allyl monomer with methyl methacrylate (MMA) and butyl acrylate (BA). Inhibitory activities of the copolymers against marine fouling organisms were also investigated. Results revealed that the copolymers exhibit a clear synergistic inhibitory effect on the growth of three seaweeds: *Chlorella*, *Isochrysis galbana* and *Chaetoceros curvisetus*, respectively, and three bacteria, *Staphylococcus aureus*, *Vibrio coralliilyticus* and *Vibrio parahaemolyticus*, respectively. In addition, the copolymers exhibited excellent inhibition against barnacle larvae. Marine field tests indicated that the resins exhibit outstanding antifouling potency against marine fouling organisms. Moreover, the introduction of the heterocyclic group led to the significantly enhanced antifouling activities of the resins; the addition of the heterocyclic unit in copolymers led to better inhibition than that observed in the case of the resin copolymerized with only the benzoisothiazolinone active monomer.

Introduction

Biofouling, which is the undesired growth and attachment of marine organisms on a solid surface of marine artificial structures (*i.e.*, docks, marine pipelines and cages) or hulls, typically causes serious problems in marine-related industries and activities.[1] For example, large-scale fouling organisms adhered onto vessels in the ocean increase the weight, reduce travelling speed and increase energy consumption;[2–4] in addition, these organisms corrode vessels, introduce invasive species and cause other ecological damage.[5–9] A number of antifouling treatment methods have been developed to prevent the adhesion of marine fouling organisms; the most efficient method to prevent marine biofouling is to paint marine coatings on a solid surface; in this way, antifouling compound molecules (biocides) are released in a controlled manner to restrain the growth of adhered organisms. Currently, chemical treatments or biocides are the widely used antifoulants for preventing and controlling the marine biofouling.[10]

Conventionally, organotin self-polishing coatings are effective in control marine biofouling. However, these coatings were prohibited in 2008 due to their adverse effects on the marine ecological environment and human health; hence, environment-friendly antifouling paints are in high demand.[11–13] At present, commercial coatings containing a large number of cuprous oxide are used, but the release of copper ions will accumulate in marine organisms and have a negative impact on the ecological environment. Therefore, self-polishing antifouling coatings based on zinc polyacrylate, copper polyacrylate and polysilyl acrylate have been widely used.[14–16] This type of coating is mainly suitable for ocean going ships, and its antifouling performance is highly dependent on sailing time and ship speed. For further improve the antifouling performance and environmental protection performance, grafted antifouling functional group antifouling material,[17] amphiphilic polymer-based antifouling material,[18] biodegradable polymer-based antifouling material,[19,20] main chain degradable self-polishing antifouling materials,[21,22] low surface energy antifouling materials,[23,24] bionic antifouling materials,[25,26] and nanocomposite antifouling materials[27–30] have become current research hotspots. It should be pointed out that most of the various technologies are currently in the laboratory research stage and have excellent anti-pollution effects, but they are still

[a]*Key Laboratory of Green Catalysis and Reaction Engineering of Haikou, College of Science, Hainan University, Haikou 570228, P. R. China. E-mail: dmmc2017@163.com; yangjxmail@hainanu.edu.cn*

[b]*Hainan Provincial Fine Chemical Engineering Research Center, Hainan University, Haikou, 570228, P. R. China*

† Electronic supplementary information (ESI) available. See DOI: 10.1039/d1ra01826d

facing some difficulties in practical application. For example, the service life, the exudation rate of antifoulant and whether it is friendly to the environment, *etc.*

The author is currently focusing on antifouling materials grafted with antifouling functional groups. The key aspect in the development of environment-friendly antifouling coatings is the innovation of the polymer resin and antifoulant. Polyacrylate is widely used in coatings because of its excellent film-forming properties and mechanical properties, fast drying, and convenient construction. Hence, a coating system based on an acrylic resin bearing an antifouling agent *via* copolymerization is critical to its performance and service life.[31–34]

Isothiazolinone compounds are a key component in bactericides, pesticides and medical and health products due to their strong antibacterial ability, low toxicity and good compatibility with other additives.[35–38] For example, 4,5-dichloro-2-*n*-octyl-4-isothiazolin-3-one (DCOIT) has been reported as a green marine antifoulant,[39] and DCOIT derivatives of benzoisothiazolinone also have been reported to exhibit a strong inhibitory effect against *Escherichia coli*, *Saccharomyces cerevisiae* and *Aspergillus niger*.[40,41] *N*-Carboxylic acid derivatives of 1,2-benzisothiazol-3(2*H*)-one (BIT) exhibit good broad-spectrum antifungal activity against *Candida* and *Aspergillus*.[42] This type of antifoulant is grafted onto polyacrylate, and the release of the antifoulant is carried out through the chemical method of "hydrolysis and diffusion" to avoid local antifoulant burst release, which is beneficial to improve the utilization rate of antifoulant, thereby increasing the antifouling performance of coatings.

To develop eco-friendly marine antifouling systems with a good antifouling performance, a series of novel grafted copolymers were prepared by the polymerization of alkenyl benzoisothiazolinone with an acrylic ester monomer and subsequent modification by alkenyl heterocyclic monomers (Scheme 1). In addition, bioactivities of the copolymers were evaluated, and their practical applications in the marine field also were investigated for further confirming the antifouling performance of the copolymeric coatings.

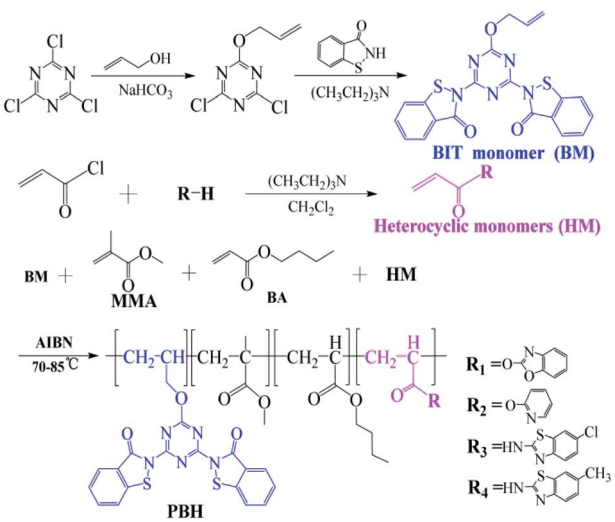

Scheme 1 Synthetic routes of acrylate triazinecopolymers.

Experimental

Synthesis of BIT monomer

First, allyl alcohol (10 mL), cyanuric chloride (1.85 g, 10 mmol) and sodium hydrogen carbonate (1.05 g, 12.5 mmol) were sequentially added in a 50 mL two-necked flask, and the mixture was stirred for 0.5 h in an ice-water bath, followed by stirring at room temperature for 3 h. Second, the reaction mixture was extracted using ethyl acetate (40 mL) and washed three times with water. The organic phase was dried over anhydrous magnesium sulfate and filtered to afford a colorless transparent filtrate for the next step. In another flask, BIT (3.02 g, 20 mmol) was added to the above solution; after stirring for 1 h, triethylamine (3 mL) was added, and the solution was stirred at room temperature for another 4 h. The reaction mixture was filtered, and the filtrate was washed three times with water. The ester layer was dried over anhydrous magnesium sulfate and concentrated to obtain monomer **BM**.

BM: yellow solid powder; 89.8% yield, melting point: 110.5–112.3 °C. ^{1}H NMR (400 MHz, $CDCl_3$), δ 7.82 (d, J = 8.4 Hz, 2H, PhH), 7.74 (d, J = 8.0 Hz, 2H, PhH), 7.51 (t, J = 7.2 Hz, 2H, PhH), 7.37 (t, J = 8.0 Hz, 2H, PhH), 5.85–5.76 (m, H, –CH═), 5.16–5.11 (m, 2H, ═CH_2), 4.71 (d, J = 6.0 Hz, 2H, CH_2). IR (KBr), ν (cm^{-1}): 3058, 2927, 2854, 1587, 1496, 1441, 1325, 967, 925, 738 cm^{-1}.

Synthesis of heterocyclic monomers

Heterocyclic monomer compounds were synthesized by the condensation of 2-hydroxyl- or 2-amino-substituted heterocycles with acryl chloride. The general procedure was as follows: first, a 50 mL two-necked flask was placed in an ice-water bath, followed by the addition of heterocyclic amines or phenols (0.01 mol), dichloromethane (20 mL) and triethylamine (1.38 mL). Second, a mixture of acryloyl chloride (1.09 g, 0.012 mol) and dichloromethane (20 mL) was slowly added dropwise, and the mixture was reacted at room temperature for 6–12 h after the end of addition. The solution was washed three times with water. The organic phase was dried over anhydrous magnesium sulfate and evaporated under reduced pressure to afford heterocyclic monomer compounds **HM**.

2-Acryloxybenzoxazole. ^{1}H NMR (400 MHz, DMSO-d_6), δ 8.03–8.00 (m, 1H, PhH),7.50 (dd, J = 17.2, 10.4 Hz, 1H, –CH═), 7.47–7.45 (m, 1H, PhH),7.37–7.31 (m, 2H, PhH), 6.64–6.59 (dd, J = 17.2, 1.2 Hz, 1H, ═CH_2(Z)), 6.20–6.17 (dd, J = 10.4, 1.2 Hz, 1H, ═CH_2(E)). IR (KBr), ν (cm^{-1}): 3056, 1748, 1704, 1623, 1600, 1481, 1251, 1145, 972, 918, 748 cm^{-1}.

2-Acryloxypyridine. ^{1}H NMR (400 MHz, DMSO-d_6), δ 8.03–8.01 (m, 1H, PhH), 7.54–7.47 (dd, J = 17.2, 10.4 Hz, 1H, –CH═), 7.47–7.44 (m, 1H, PhH), 7.37–7.31 (m, 2H, PhH), 6.64–6.59 (dd, J = 17.2, 1.2 Hz, 1H, ═CH_2(Z)), 6.20–6.17 (dd, J = 10.4, 1.2 Hz, 1H, ═CH_2(E)). IR (KBr), ν (cm^{-1}): 3074, 1706, 1641, 1541, 1465, 1215, 1157, 983, 918 cm^{-1}.

2-Acrylamide-6-chlorobenzothiazole. ^{1}H NMR (400 MHz, DMSO-d_6), δ 12.72 (s, H, –NH), 8.18 (d, J = 2.0 Hz, 1H, PhH), 7.78 (d, J = 8.8, Hz, 1H, PhH), 7.49 (dd, J = 8.8, 2.0 Hz, 1H, PhH), 6.64–6.57 (dd, J = 17.2, 10.0 Hz, 1H, –CH═), 6.52–6.47 (dd, J = 17.2, 1.6 Hz, 1H, ═CH_2(Z)), 6.02–5.99 (dd, J = 10.0, 1.2 Hz, 1H, ═CH_2(E)). IR (KBr), ν (cm^{-1}): 3452, 3031, 1697, 1623, 1595, 1535, 1442, 1400, 987, 900, 883, 804 cm^{-1}.

2-Acrylamide-6-methylbenzothiazole. ^{1}H NMR (400 MHz, DMSO-d_6), δ 12.55 (s, H, –NH), 7.81 (s, 1H, PhH), 7.74(d, J = 8.8 Hz, 1H, PhH), 7.29 (dd, J = 8.8, Hz, 1H, PhH), 6.60 (dd, J = 18.4, 10.0 Hz, 1H, –CH═), 6.47 (dd, J = 18.4, 2.0 Hz, 1H, ═$CH_2(Z)$), 5.98 (dd, J = 10.0, 2.0 Hz, 1H, ═$CH_2(E)$), 2.44 (s, 3H, CH_3). IR (KBr), ν (cm^{-1}): 3434, 3055, 2921, 2854, 1695, 1627, 1606, 1552, 1461, 1404, 983, 902 881, 791 cm^{-1}.

Synthesis of copolymer PBHs

Scheme 1 shows the synthetic pathways of the target copolymer PBHs comprising **BM**, MMA, BA and **HM** monomers. Typically, MMA, BA, **BM**, **HM** and AIBN (0.5–1.0 wt% of total monomers) were dissolved in a mixture of xylene and *n*-butanol in a three-necked flask with a magnetic stirring bar and equipped with a reflux condenser. With the increase in the temperature to 70–85 °C, polymerization was performed under nitrogen for 6–10 h, affording the target copolymer. The reaction solution was removed at certain intervals for examining the monomer consumption with reaction time.

Structural measurements

^{1}H NMR spectra (400 MHz) were recorded on a Bruker AVANCE instrument using $CDCl_3$ or DMSO-d_6 as the solvent at room temperature. Fourier transform infrared (FTIR) spectra of polymer films cast onto potassium bromide plates were recorded using a Bruker TENSOR 27 FTIR spectrometer. Gel permeation chromatography (GPC) curves were recorded on a United States Waters 1515 apparatus (with THF as the eluent at a flow rate of 1.00 mL min^{-1} at 35 °C). The GPC instrument was calibrated using polystyrene (PS) standards.

DSC curves were measured on a Q100 SDT thermogravimetric analyzer (TA Inc., USA) by placing 10–20 mg of the liquid polymer sample in an alumina crucible under N_2 at a heating rate of 10 °C min^{-1} and a heating range of 25–130 °C. The T_g value of the polymer was obtained by DSC characterization.

TGA curves were recorded on a Q600 SDT thermogravimetric analyzer (TA Inc., USA) by placing 5–10 mg of the liquid polymer sample in an alumina crucible under N_2 at a heating rate of 10 °C min^{-1} and a temperature range of 20–600 °C. TGA was employed to analyze the thermal stability of polymers.

Weight loss measurements

Each copolymer liquid was added dropwise on a slide glass surface, followed by naturally drying to constant weight. Next, the plate was placed into a glass cup with fresh seawater and changed every week. The plate was taken out, rinsed with deionized water and dried to constant weight at room temperature. The weight loss rate was calculated as follows:

$$\text{Mass loss wt\%} = \frac{W_0 - W_t}{W_0 - W_{kb}} \times 100\% \quad (1)$$

where, W_0 is the weight of the initial sample plate, and W_t and W_{kb} are the weights of the target sample plate and blank plate after the interval time t, respectively. Three independent experiments were repeated for each sample.

Contact angle test

Take the copolymer and brush it on a glass slide and dry at room temperature. Use the SL200KB interfacial tension meter of Shanghai SUOLUN Company to characterize, test the change of the contact angle of the ultrapure water on the surface of the polymer after hydrolysis. The amount of ultrapure water used is 2 μL each time, and each polymer must be tested in three different places and averaged.

Algae inhibition measurements

Chlorella, *Isochrysis galbana* and *Chaetoceros curvisetus* were provided by the algae culture group of the Ocean College of Hainan University. Three different algae were selected for testing to show the universality of the copolymer's inhibition of algae. The maximum absorption wavelength of each solution of marine algae was obtained by scanning the ultraviolet wavelengths using a UV-visible spectrophotometer, and the corresponding values of *Chlorella*, *I. galbana* and *C. curvisetus* were 685, 485 and 685 nm, respectively. The concentration of the algae liquid with different absorbance values was measured by hemocytometer counting, and each group was measured three times to obtain an average concentration of the algae solution. The absorption value of each dilution was measured at the maximum absorption wavelength. A standard curve was plotted with the absorption value and marine algae concentration as the abscissa and ordinate, respectively. Data of the absorbance and algae liquid concentration were linearly simulated (Fig. 1).

The resin PBH was separately brushed on a surface of a glass panel (75 mm × 25 mm × 1.2 mm), and the commercial acrylic resin without the BIT component was used as the control group. The resin panels were naturally dried at room temperature. The algae solution was diluted with the nutrient solution so that the

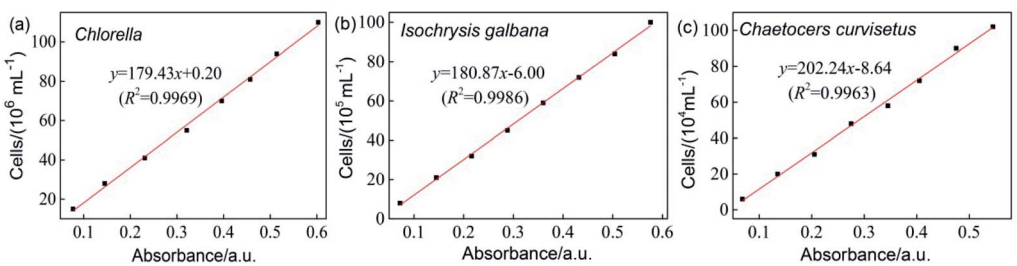

Fig. 1 Working curves between absorbance and concentration of *Chlorella* (a), *Isochrysis galbana* (b) and *Chaetocers curvisetus* (c).

absorption value was between 0.05 and 0.1; the resin panel was placed into the algae solution, and the beaker was sealed with a semi-permeable membrane. Each of the samples and control group were measured every 24 h, and the absorbance was recorded. In accordance with the absorbance-concentration curve for the algae dilution, the corresponding concentration of algae was calculated, and the concentration–time curves of algae were plotted.[43,44]

Antibacterial activity test

Gram-negative bacteria are predominant in seawater, and *Vibrio* is a typical marine bacteria. Ocean-going ships dock in the inner bay area. Generally, both positive and negative bacteria exist in the inner bay area. *S. aureus* is a positive bacteria, and it is necessary to choose *S. aureus* for antibacterial test. The selection of these three kinds of bacteria is to show the universality of the copolymer to inhibit negative bacteria and positive bacteria. *S. aureus*, *V. coralliilyticus* and *V. parahaemolyticus* were provided by the Marine Drugs Research Laboratory of Hainan University. The antibacterial property of the target resin was investigated by the absorbance method. Tryptone soybean broth (TSB) was the culture medium for *S. aureus*, and the 2216E liquid culture medium was the culture media for *V. coralliilyticus* and *V. parahaemolyticus*. The resin-coated cell culture plates were sterilized by ultraviolet light for 2 h before the test. Then, 5 mL of the liquid culture solution and 50 μL of the cultured bacterial solution were separately added to each well and cultured in an incubator at 37 °C. The absorbance values of the cells were measured at 600 nm at time intervals of 2 h, 4 h, 6 h, 8 h, 10 hand 12 h, and absorption values of the bacterial solution in the culture solution were observed.[45,46]

Barnacle larvae inhibition test

Barnacles are typical large fouling organisms. It is necessary to test the copolymer for its inhibitory activity. Adult barnacles were collected near Haikou Bay in Hainan Island. After the adult barnacles were washed with seawater, the elder barnacles were selected and dried in a dark place for 12 h. Then, the barnacles were immersed in fresh seawater and exposed to light. As the phototaxis of barnacle larvae was under sunlight, a large number of barnacle larvae hatched from adult soon and swam to the light side. First, 1.0 mL of the copolymer was added into each Petri dish, spread out and dried in air at room temperature. Next, quantitative barnacle larvae were carefully drawn up using a pipette, added into the Petri dish and mixed with 30 mL of fresh seawater at room temperature. Each Petri dish contained 15 barnacle larvae, and the survival of barnacle larvae was observed and recorded by a stereo-microscope at 12 h and 24 h. When barnacle larvae greater than 15 s, they were considered to be dead. The death larvae were removed in time to ensure the accuracy of further experiments.[47,48] Each copolymer was tested three times and averaged while using the blank as the control group.

Marine field tests

Marine field tests were performed from August to October in the South China Sea (110.19′E, 20.1′N) in China, where the surface water temperature ranges from 25 to 28 °C. First, low-carbon steel plates ($300 \times 200 \times 3$ mm^3) were polished twice with sandpaper (120 mesh) to remove rust, cleaned with pure water and ethanol and then painted with two layers of acrylic resin. Second, the copolymer samples were brushed twice on the acrylic resin surface of the steel panels and marked. After the paint dried, and it was naturally cured in a well-ventilated place, the panels were immersed into seawater at a depth of 0.5–1.0 m. Meanwhile, blank samples KB (acrylic resin) were used as the control group. After a 1 month interval, the panels were removed from the sea and carefully washed with seawater to remove the floating objects and photographed, followed by immediately placing them back in the seawater to continue marine field tests. The antifouling activity was evaluated according to ASTMD6990-05 (2011).[49]

Results and discussion

Characterization of copolymers

The antifouling resins of copolymers grafted with heterocyclic monomers have not been reported in the literature. The molecular weights of the copolymers PBH were ~10 000 (Table 1). The number-average molecular weights (M_n) ranged from 9858 to 13 226, while the weight-average molecular weights (M_w) ranged from 10 830 to 13 592, both of which were not quite different. The poly dispersity indexes (PDIs) of the copolymers were between 1.01 and 1.14, indicative of a relatively uniform molecular-weight distribution. Each copolymer exhibited a single glass transition temperature (T_g), suggesting that all of the PBHs are random copolymers. A melting peak was not

Table 1 Molecular compositions and characterizations of copolymer

	Ratio of monomer (%)				
Samples	**BM**/MMA/BA/**HM**	M_n (g mol^{-1})	M_w (g mol^{-1})	PDI	T_g (°C)
PBH1	5/47.5/47.5/0	10 658	11 011	1.03	52.36
PBH2	10/45/45/0	10 728	11 110	1.04	60.21
PBH3	15/42.5/42.5/0	10 678	10 947	1.03	55.14
PBH4	20/40/40/0	11 357	11 545	1.02	78.34
PBH5	20/32.5/32.5/15 (R_1)	11 609	11 772	1.01	31.29
PBH6	20/32.5/32.5/15 (R_2)	10 679	10 830	1.01	54.40
PBH7	20/32.5/32.5/15 (R_3)	12 077	12 681	1.05	57.80
PBH8	20/32.5/32.5/15 (R_4)	10 611	11 390	1.07	57.18

observed in DSC curves, indicative of the amorphous nature of the copolymers. The successful copolymerization of PBH polymers was confirmed by FTIR and ^{1}H NMR (Fig. 2).

PBH4 was selected as a representative copolymer for comparison with **BM** to verify whether copolymerization was complete (Fig. 2a). In the FTIR spectrum of **PBH4**, a clear absorption peak was not observed at 3100 to 3000 cm^{-1} and 995 to 905 cm^{-1} (green frame), indicating that the carbon–carbon double bond does not exist and that the carbon–carbon double bond of each monomer in the copolymer is completely reacted. The absorption peaks at 1560 and 1595 cm^{-1} indicate the presence of the benzene ring. The absorption peak at 759 cm^{-1} indicates that an *ortho*-disubstituted benzene ring is still present. The newly observed absorption peaks at 1731 and 1680 cm^{-1} corresponded to the presence of an ester group, while the absorption peak at 1380 cm^{-1} corresponded to the methyl group. Except for the carbon–carbon double bond, the functional groups of each monomer in the copolymer are present.

Fig. 2b shows the ^{1}H NMR spectrum of the copolymer **PBH4**. The copolymer contained a small amount of Ph–H, and multiple sets of characteristic peaks at δ = 7.38–8.27 were observed, corresponding to the peaks characteristic of H in Ph–H. A group of characteristic peaks was observed at δ = 4.68–4.78, corresponding to the peaks characteristic of OCH_3 in the **BM** monomer. In the copolymer, C–H was connected to the ester group in the butyl ester compound, and the peak corresponding to the methyl ester compound was observed in the unshielded region of the ether oxygen atom; this peak position shifted to low field, and two sets of peaks were observed at δ = 3.43–4.12, corresponding to the peak characteristic of C–H in $RCOOCH_2R$ and that characteristic of C–H in $RCOOCH_3$. The copolymer comprised a large amount of C–H, and multiple sets of characteristic peaks were observed at δ = 0.75–1.65, corresponding to the peaks characteristic of H in CH_3 and CH_2. The above analysis confirmed the copolymer **PBH4** structure. All of the structural characterization methods validate that copolymerization is completed and that each monomer participates in polymerization.

Thermal stability analysis of PBHs

Fig. 2c shows the thermal stability analysis of PBHs. With the increase in the temperature, the weight loss of the polymer was categorized into two stages. The first stage occurred at 150–300 °C, with a small weight loss rate, possibly related to the decomposition of unreacted small molecular substances. The second stage occurred at 300–500 °C, with significant molecular-weight loss, indicative of the thermal decomposition of the polymer.

Weight loss rate measurements

The weight loss rate was measured for investigating the hydrolytic release of the antifoulant in the grafted resin (Fig. 2d). When the plates were immersed in seawater, the mass of the coatings started to decrease due to the hydrolysis of the ester bond of the monomers. By the introduction of the heterocyclic monomer, the loss rate increased, and after copolymerization with various monomers, the hydrolysis rate of the resins changed.

In the initial days, the mass loss rate ranged from 0.015 to 0.025 mg cm^{-2} d^{-1}. After 90 days, the mass lost rate tended to be stable at 0.01–0.015 mg cm^{-2} d^{-1}, indicative of the sustained release of the graft coating. In particular, the mass loss rate of **PBH8** was greater than those of other samples, with an average rate of 0.015 mg cm^{-2} d^{-1}, and **PBH7** exhibited the lowest mass loss, with an average rate of 0.01 mg cm^{-2} d^{-1}.

Contact angle test

Fig. 2e shows the change of the contact angle of the polymer surface with the immersion time after the samples with different monomer contents are immersed in fresh seawater. The contact angle test can reflect the changes in the hydrophilicity and hydrophobicity of the surface of the material, and further reflect the changes in the chemical structure of the

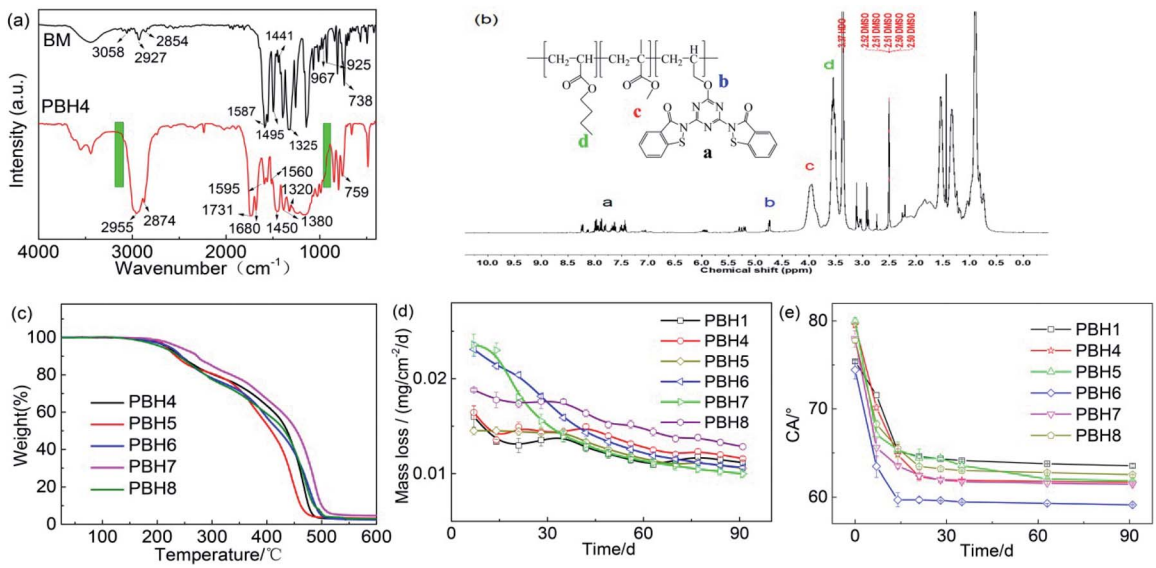

Fig. 2 (a) FT-IR spectra of **BM** and copolymer **PBH4**, (b) ^{1}H NMR spectrum of copolymer **PBH4**, (c) trend of thermal stability of polymers, (d) hydrolysis weight loss of polymers PBH, (e) change of contact angle of polymer PBH after hydrolysis.

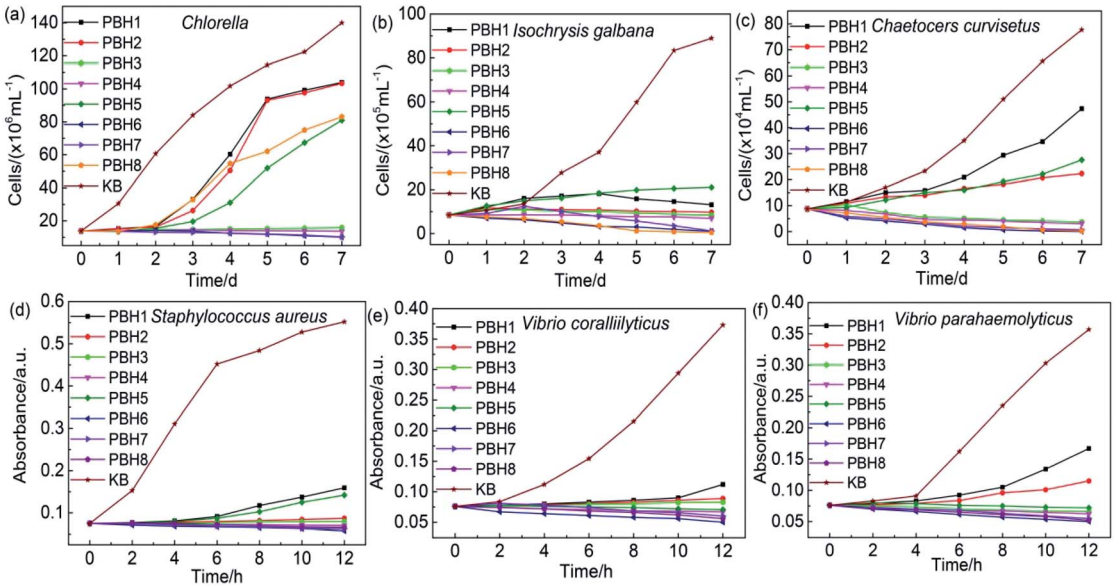

Fig. 3 (a) Inhibition of PBHs on *Chlorella*, (b) inhibition of PBHs on *Isochrysis galbana*, (c) inhibition of PBHs on *Chaetocers curvisetus*, (d) antibacterial activity of PBHs against *Staphylococcus aureus*, (e) antibacterial activity of PBHs against *Vibrio coralliilyticus*, (f) antibacterial activity of PBHs against *Vibrio parahaemolyticus*.

surface. At 0 days, the contact angle of the copolymer **PBH4** with 20% by weight of BIT monomer is greater than that of **PBH1** with 5% by weight due to the side chain contains hydrophobic acrylate groups. As the content of side chains increases, the static water contact angle also increases. It shows that as the content of side chains increases, the content of side chains that migrate to the surface of the sample also increases. After introducing different heterocyclic monomers into the copolymer, the contact angle of the resin sample decreases with the increase of immersion time. After 21 days, the static water contact angle became stable. This is because after the superficial acrylate monomer, **BM** monomer, and heterocyclic monomer are hydrolyzed, OH or COOH is generated, so that the superficial coat of the polymer becomes more hydrophilic and the contact angle becomes smaller.

Inhibition of marine algae growth

The inhibition rate was calculated from the algae absorbance–concentration working curve. With time and algal concentration as the horizontal and longitudinal axes, respectively, the time was set at 1 d, 2 d, 3 d, 4 d, 5 d, 6 d and 7 d. Fig. 3 shows the inhibition curve of PBHs on the growth of three marine algae (*i.e.*, *Chlorella*, *I. galbana* and *C. curvisetus*, respectively), and Table 2 summarizes data on the 7th day.

From Fig. 3 and Table 2, the absorbance of the algal solution was linearly related to the concentration. The target copolymers exhibited certain algal inhibition activities, effectively restricting the growth of algal cells in the initial stage of passage.

The copolymer PBHs clearly inhibited the growth of *Chlorella* (Fig. 3a). At the start of cultivation, *Chlorella* reproduced slowly in the solution when immersing the target copolymers, followed by the favourable inhibition effect compared to the control group. As the cultivation continued, some of the target copolymers suppressed the growth of *Chlorella* to some extent after 2 days. The compounds polymerized with the monomers **BM** and **HM** clearly exhibited a better inhibitory activity against *Chlorella* than that observed for compounds copolymerized only with the **BM** monomer, and with the increase in the grafted ratio of BIT, the potency of inhibition increased. Especially, **PBH6** and **PBH7**, polymerized with 2-acryloxypyridine and 2-acrylamide-6-chlorobenzothiazole, respectively, exhibited significantly improved inhibitory activities against *Chlorella*, with corresponding average rates of 92.81% and 92.68%, almost inhibiting the growth of *Chlorella*. **PBH5** and **PBH8**, which were polymerized with 2-acryloxybenzoxazole and 2-acrylamide-6-methylbenzothiazole, respectively, exhibited a low inhibitory activity with corresponding average rates of 42.17% and 40.64%; these rates are considerably less than those of **PBH6** and **PBH7**.

Table 2 Inhibition rate of copolymer PBHs against the growth of algae

	Inhibition rate (7 days)/%		
Polymers	*Chlorella*	*Isochrysis galbana*	*Chaetocers curvisetus*
PBH1	25.77%	85.19%	39.04%
PBH2	26.15%	89.06%	71.30%
PBH3	88.71%	90.48%	95.24%
PBH4	90.24%	92.11%	96.02%
PBH5	42.17%	76.25%	64.54%
PBH6	92.81%	98.82%	99.93%
PBH7	92.68%	98.61%	99.15%
PBH8	40.64%	99.43%	99.67%

Compared to the control group, the target copolymers exhibited excellent inhibitory activities against *I. galbana* (Fig. 3b). Notable reproduction was not observed in the first 2 days, and the algae concentration remained almost unchanged. When the seaweed solution was cultured for 7 days, all target copolymers were observed to completely inhibit the growth of *I. galbana*. **PBH6**, **PBH7** and **PBH8**, which were polymerized with 2-acryloxypyridine, 2-acrylamide-6-chlorobenzothiazole and 2-acrylamide-6-methylbenzothiazole, respectively, exhibited outstanding inhibitory activities against *I. galbana*; their corresponding average rates were 98.82%, 98.61% and 99.43%, almost inhibiting the growth of *I. galbana*. On the 1st day, the algae concentrations considerably decreased. However, **PBH5** polymerized with 2-acryloxybenzoxazole exhibited a poor inhibitory activity against *I. galbana*, with an average rate of 76.25%, compared to the other copolymers polymerized with the **HM** monomer.

Fig. 3c shows the inhibitory activities of the copolymer PBHs on the growth of *C. curvisetus*. All of the BIT polymeric derivatives exhibited a better inhibitory effect than that of the control group on the reproduction of *C. curvisetus*. For the cultivation of the algae on the 1st day, the *C. curvisetus* concentrations did not significantly differ between the algae solutions of the polymeric derivatives.

With the continuation of the culture process, inhibitory activities of the copolymers PBH exhibited notable changes.

The resins polymerized with the monomer **HM** exhibited the best inhibitory performance. Particularly, **PBH6**, **PBH7** and **PBH8** exhibited outstanding inhibitory activities against *C. curvisetus*, with corresponding average rates of 99.93%, 99.15% and 99.67%, completely inhibiting the growth of *C. curvisetus*. Among the heterocyclic resins, only **PBH5** exhibited a poor performance.

The mechanism of inhibiting the growth of algae is: polymer hydrolysis will produce and release small molecular compounds. It enters algae cells more easily, destroying the structure and function of organelles. The algae cells gradually disappear, showing an inhibitory effect on the algae.

Inhibition of bacterial growth

Antibacterial abilities of copolymer PBHs were investigated. The absorbance of the bacterial solution at different times was measured to quantify the inhibition potency of the copolymer against bacterial growth. The inhibition rate was calculated according to the absorbance–concentration working curve. With the time and algal concentration as the horizontal and longitudinal axes, respectively, the action time was set to 2 h, 4 h, 6 h, 8 h, 10 h and 12 h. Fig. 3 shows the inhibition activity of PBHs on the growth of *S. aureus*, *V. coralliilyticus* and *V. parahaemolyticus*, and Table 3 summarizes the values.

Table 3 Inhibition rate of compounds against bacterial growth

	Inhibition rate (12 h)/%		
Polymers	*Staphylococcus aureus*	*Vibrio coralliilyticus*	*Vibrio parahaemolyticus*
PBH1	77.76%	80.06%	61.29%
PBH2	92.08%	87.12%	78.06%
PBH3	93.47%	88.96%	93.87%
PBH4	95.45%	93.87%	95.05%
PBH5	81.19%	92.74%	91.94%
PBH6	97.82%	99.08%	99.03%
PBH7	96.83%	96.01%	97.42%
PBH8	96.24%	97.24%	98.39%

The copolymer PBHs clearly inhibited the reproduction of *S. aureus*, and the inhibition rate was linearly related to the BIT concentration. Among the copolymers, the resins polymerized by the addition of heterocyclic monomers, such as **PBH6**, **PBH7** and **PBH8**, exhibited better antibacterial activities (Fig. 3d).

At the beginning of cultivation, *S. aureus* reproduced slowly and exhibited good inhibition activities compared to the control group. With the continuation of cultivation, all target copolymers well suppressed the reproduction of *S. aureus* throughout the entire experimental period. The compounds polymerized with the monomers **BM** and **HM** clearly exhibited better inhibitory activities, and with the increase in the grafted ratio of BIT, the potency of inhibition increased. Especially, **PBH6**, **PBH7** and **PBH8**, which were polymerized with 2-acryloxypyridine, 2-acrylamide-6-chlorobenzothiazole and 2-acrylamide-6-methylbenzothiazole, respectively, exhibited significantly improved inhibitory activities against *S. aureus*; their corresponding average rates were 97.82%, 96.83 and 96.24%, almost inhibiting the growth of *S. aureus*. **PBH5**, which was polymerized with 2-acryloxybenzoxazole, exhibited a low inhibitory activity, with an average rate of 81.19%. Similar to the case of *S. aureus*, the growth of *V. coralliilyticus* was efficiently inhibited by the copolymers (Fig. 3e), leading to the marginal reproduction and low concentration of *V. coralliilyticus*on the 1st day. After the 7 day culture of the bacteria solution, *V. coralliilyticus* was completely blocked by the target copolymers. For instance, the **PBH6**, **PBH7** and **PBH8**, which were polymerized with 2-acryloxypyridine, 2-acrylamide-6-chlorobenzothiazole and 2-acrylamide-6-methylbenzothiazole, respectively, exhibited good inhibitory activities against *V. coralliilyticus*; their corresponding average rates were 99.08%, 96.01% and 97.24%, resulting in the complete growth cease.

Fig. 3f shows the inhibition of the PBHs on the growth of *V. parahaemolyticus*. Compared to the control group, the BIT polymeric derivatives exhibited better inhibitory activity on the reproduction of *V. parahaemolyticus*. No considerable difference in the bacterial concentrations on the 1st day. However, significant changes in the inhibitory activities were observed with the progress of the culture. The resins polymerized with the monomer **HM**, such as **PBH6**, **PBH7** and **PBH8**, exhibited good performance towards the growth inhibition of *V. parahaemolyticus*; the corresponding average rates were 99.03%, 97.42% and 98.39%, respectively. **PBH5**, with an inhibition rate of 91.94%, which was slightly less than those of other heterocyclic resins, was still a good inhibitor against *V. parahaemolyticus*.

The mechanism of inhibiting bacterial growth is: polymer hydrolysis will produce and release small molecules of BIT compounds. The S–N bond in BIT molecule breaks and forms

S–S bond with the receptor, which interact with the base on the biological protein to form a hydrogen bond. The hydrogen bond has a strong attraction and can firmly adhere to the bacterial cell, thereby destroying the structure of the DNA, unable to replicate, and ultimately leading to the death of the bacteria.

Inhibition of barnacle larvae

Fig. 4a shows the death rates of barnacle larvae caused by the various copolymer PBHs. The inhibitory ability of the copolymers containing BIT was greater than that of the contrast polyacrylic ester, and with the increase in the BIT component, the survival number of barnacle larvae gradually decreased. Thus, the introduction of a heterocyclic structure into the compounds leads to the considerable improvement in the inhibitory performance of the PBHs against barnacle larvae.

Relative to the control sample, the addition of BIT into the PBH chemical structures resulted in a higher potency inhibitory activity. By the introduction of 5% of the BIT component (**PBH1**), the inhibition rates of the barnacle larvae increased to 33.3% in 12 h and 55.6% at 24 h. In case of 10% of the BIT component (**PBH2**), the inhibition rates of the barnacle larvae increased to 37.8% in 12 h and 64.4% at 24 h. As the BIT content reached 20% (**PBH4**), the inhibition rates of the barnacle larvae increased to 62.2% in 12 h and 82.2% at 24 h. The presence of the heterocyclic ring led to the dramatic enhancement in the polymeric activity. For the copolymer grafted with 15% of 2-acrylamide-6-chlorobenzothiazole (**PBH7**), the inhibition rates of the barnacle larvae increased to 71.1% in 12 h and 91.1% at 24 h, while for the copolymer grafted with 15% of 2-acryloxypyridine (**PBH6**),the inhibition rate of the barnacle larvae increased to 80.0% in 12 h and 100.0% at 24 h.

Application on antifouling coatings

To further investigate the inhibition potency of these newly synthesized polymeric PBHs as antifouling coatings, the application performance of the copolymers was evaluated in marine field tests. Coating samples were painted on the surface of thin steel sheets and then immersed in seawater near the coast for 3 months, and the marine organisms adhered on the sheet steel were periodically recorded. For comparison, samples containing 20% BIT (**PBH4–PBH8**) were selected for application tests, and polyacrylate (**KB**) was selected as the control group for contrast. Fig. 4c shows the typical images of the tested panels after immersion in seawater.

All of the tested coatings comprising the BIT structural unit exhibited better antibiofouling activity than that of the KB control group. After immersing in seawater for 60 days, a small amount of seaweeds adhered on the coating surfaces, and rare large-scale marine organisms, including barnacles and mussels, adhered on the coatings, suggesting that copolymeric compounds can be used as outstanding antifouling coatings in boating and marine industry. On the contrary, the polyacrylate blank panel exhibited adverse fouling by marine organisms due to the covering of the surface by mussels and the growth of barnacles or oysters on the mussels.

After 90 days marine field tests, a few of the fouling organisms were observed to adhere on the BIT copolymeric coating surface. Within the organisms, most were barnacles, and few mussels were attached. On the other hand, the blank panel surface was covered by a large amount of barnacles and mussels.

The introduction of the heterocyclic unit in chemical compounds significantly enhanced the antifouling activities of

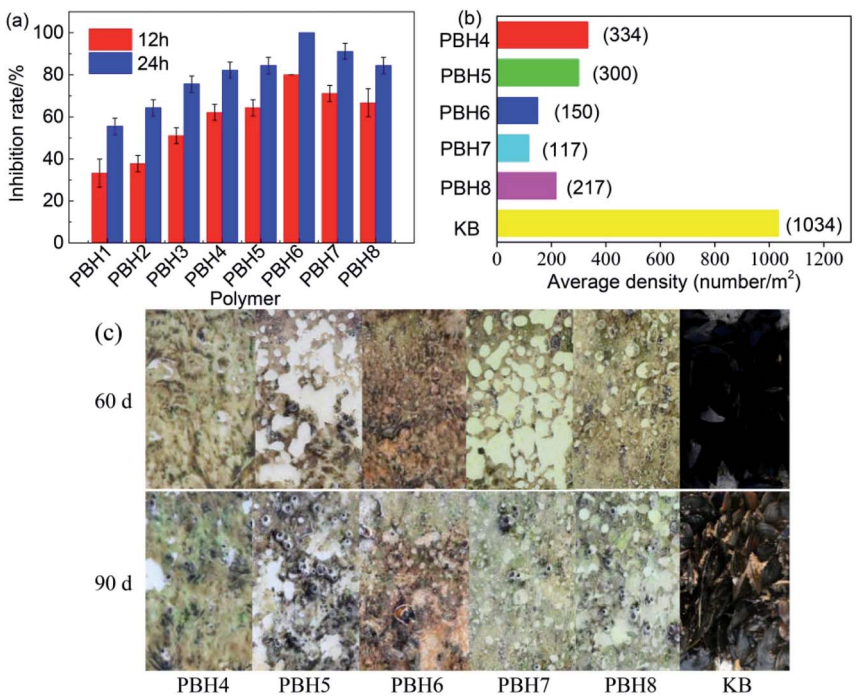

Fig. 4 (a) Inhibition rates of barnacle larva inhibited by PBHs, (b) statistical density of barnacles on marine field tests, (c) antifouling performance of the resin immersion in seawater.

the copolymeric coatings. Although a small number of barnacles were still attached on the panel surface, the coatings with the use of heterocyclic compounds were considerably better in inhibiting the marine fouling organisms than that observed for the coatings without the heterocyclic compounds. For **PBH6** and **PBH7**, which were grafted by 15% 2-acryloxypyridine or 2-acrylamide-6-chlorobenzothiazole, respectively, the antifouling abilities were better than those of non-heterocyclic compounds, and the average density of fouling organisms on the surface was less than that of **PBH4**, revealing that the presence of a heterocyclic unit on the polymer side chain increases the anti-biofouling efficiencies.

The statistical density of barnacles grown on the copolymers was analysed on the basis of the results of 90 days marine field tests (Fig. 4b). Compared to the control group **KB**, all target copolymers exhibited better antifouling properties. The average growth of barnacles on the target copolymers ranged from 117 to 334 m^{-2}, which was less than that on the control group **KB**, with an average of 1034 m^{-2}. The average densities of **PBH7** and **PBH4**, among PBH panels, were 117 m^{-2} and 334 m^{-2}, respectively. Our studies indicated that the addition of the heterocyclic monomers in the polymeric structure leads to an interesting synergistic effect.

Conclusions

Eight grafted acrylic polymeric resins containing BIT and heterocyclic functional structures were synthesized by the copolymerization of acrylate with benzoisothiazolinone-*s*-triazine and the heterocyclic monomer. The bioactivities of the copolymers were examined, such as algae inhibitory activity, antibacterial activity, barnacle larvae inhibitory activity, which were subsequently applied as antifouling coatings. The results reveal that all copolymers exhibit clear biological activities and that the introduction of a heterocyclic unit leads to the significant enhancement of antifouling activities. Coatings copolymerized with the heterocyclic compound exhibited more evident inhibitory effects on marine fouling organisms than that exhibited by the copolymers without the heterocyclic compound coating. The synthesis of such grafted copolymers will lay a foundation for further study of anti-fouling resins.

Conflicts of interest

There are no conflicts to declare.

Acknowledgements

This research was funded by Scientific Research Project of Sanya Yazhouwan Science and Technology City Administration Bureau (SKJC-2020-01-004) and the National Natural Science Foundation of China (51663009, 52063011).

Notes and references

1 M. Lejars, A. Margaillan and C. Bressy, *Chem. Rev.*, 2012, **112**, 4347–4390.
2 M. P. Schultz, *Biofouling*, 2007, **23**, 331–341.
3 M. A. Champ, *Sci. Total Environ.*, 2000, **258**, 21–71.
4 F. Pearce, Offshore petroleum, in *Bio-fouling problems and solutions [M]*, The University of New South Wales, Australia, 1994, pp. 19–31.
5 R. G. J. Edyvean, L. A. Tery and G. B. Pieken, *Int. Biodeterior.*, 1985, **21**, 277–284.
6 J. E. Gittens, T. J. Smith, R. Suleiman, *et al.*, *Biotechnol. Adv.*, 2013, **31**, 1738–1753.
7 J. M. Drake and D. M. Lodge, *Aquat. Invasions*, 2007, **2**, 121–131.
8 K. Reise, S. Gollasch and W. J. Wolff, *Helgolander. Mar. Res.*, 1998, **52**, 219–234.
9 R. F. Piola, K. A. Dafforn and E. L. Johnston, *Biofouling*, 2009, **25**, 633–644.
10 C. M. Kirschner and A. B. Brennan, *Annu. Rev. Mater. Res.*, 2012, **42**, 211–229.
11 K. V. Thomas and S. Brooks, *Biofouling*, 2010, **26**, 73–88.
12 D. M. Yebra, S. Kiil and K. Dam-Johansen, *Prog. Org. Coat.*, 2004, **50**, 75–104.
13 J. A. Callow and M. E. Callow, *Nat. Commun.*, 2011, **2**, 244.
14 Y. Yonehara, H. Yamashita, C. Kawamura and K. Itoh, *Prog. Org. Coat.*, 2001, **42**, 150–158.
15 R. Chen, Y. Li, T. Liang, H. Yang and K. Takahashi, *RSC Adv.*, 2017, **7**, 40020–40027.
16 I. Omae, *Appl. Organomet. Chem.*, 2010, **17**, 81–105.
17 K. Feng, C. Ni, L. Yu, W. Zhou and X. Li, *Colloids Surf., B*, 2019, **184**, 110518.
18 C. B. Kristalyn, X. Lu, C. J. Weinman, C. K. Ober, E. J. Kramer and Z. Chen, *Langmuir*, 2010, **26**, 11337.
19 X. Zhou, Q. Y. Xie, C. F. Ma, Z. J. Chen and G. Z. Zhang, *Ind. Eng. Chem. Res.*, 2015, **54**, 9559.
20 S. Chen, C. Ma and G. Zhang, *Prog. Org. Coat.*, 2016, **104**, 58–63.
21 C. Ma, W. Xu, J. Pan, Q. Xie and G. Zhang, *Ind. Eng. Chem. Res.*, 2016, **5**, 11495–11501.
22 Q. Xie, C. Ma, G. Zhang and C. Bressy, *Polym. Chem.*, 2018, **9**, 1448–1454.
23 L. Xiao, J. Li, S. Mieszkin, A. D. Fino and P. A. Levkin, *ACS Appl. Mater. Interfaces*, 2013, **5**, 10074–10080.
24 A. Beigbeder, P. Degee, S. L. Conlan, R. J. Mutton, A. S. Clare, M. E. Pettitt, M. E. Callow, J. A. Callow and P. Dubois, *Biofouling*, 2008, **24**, 291–302.
25 C. M. Magin, S. P. Cooper and A. B. Brennan, *Mater. Today*, 2010, **13**, 36–44.
26 T. S. Wong, S. H. Kang, S. Tang, E. J. Smythe, B. D. Hatton, A. Grinthal and J. Aizenberg, *Nature*, 2011, **477**, 443–447.
27 M. S. Selim, M. A. Shenashen, A. Elmarakbi, A. El-Saeed, M. M. Selim and S. A. El-Safty, *RSC Adv.*, 2017, **7**, 21796–21808.
28 M. S. Selim, M. A. Shenashen, S. A. El-Safty, S. A. Higazy and A. Elmarakbi, *Prog. Mater. Sci.*, 2017, **87**, 1–32.
29 M. S. Selim, M. A. Shenashen, A. Elmarakbi, N. A. Fatthallah, S. I. Hasegawa and S. A. El-Safty, *Chem. Eng. J.*, 2017, **320**, 653–666.
30 N. A. Fatthallah, M. S. Selim, S. Safty, M. M. Selim and M. A. Shenashen, *Mater. Sci. Eng., C*, 2021, **122**, 111844.

31 C. F. Ma, L. G. Xu, W. T. Xu and G. Z. Zhang, *J. Mater. Chem. B*, 2013, **1**, 3099–3106.
32 J. L. Ma, C. F. Ma, Y. Yang, W. T. Xu and G. Z. Zhang, *Ind. Eng. Chem. Res.*, 2014, **53**, 12753–12759.
33 W. T. Xu, C. F. Ma, J. L. Ma, T. S. Gan and G. Z. Zhang, *ACS Appl. Mater. Interfaces*, 2014, **6**, 4017–4024.
34 J. H. Yao, S. S. Chen, C. F. Ma and G. Z. Zhang, *J. Mater. Chem. B*, 2014, **2**, 5100–5106.
35 S. Abdel-Sattar and H. Elgazwy, *Tetrahedron*, 2003, **34**, 7445–7463.
36 F. Clerici, M. L. Gelmi, S. Pellegrino and D. Pocar, Chemistry of Biologically Active Isothiazoles, *Bioactive Heterocycles III*, September, 2009, pp. 179–264.
37 C. C. Cutri, A. Garozzo, M. A. Siracusa, *et al.*, *Bioorg. Med. Chem.*, 1999, **7**, 225–230.
38 R. V. Kaberdin and V. I. Potkin, *Russ. Chem. Rev.*, 2002, **71**, 673–694.
39 S. N. Lewis, G. A. Miller and A. B. Law. Certain 2-carbamoyl-3-isothiazolenes [P], *US Pat.*3523121, 1970-04-08.
40 P. J. Collier, A. J. Ramsey, P. Austin, *et al.*, *J. Appl. Bacteriol.*, 1990, **69**, 569–577.
41 P. Vicini, F. Zani and P. Cozzini, *Eur. J. Med. Chem.*, 2002, **37**, 553–564.
42 D. Dou, D. Alex, B. Du, *et al.*, *Bioorg. Med. Chem.*, 2011, **19**, 5782–5787.
43 F. Wan, X. Pei, B. Yu, *et al.*, *ACS Appl. Mater. Interfaces*, 2012, **4**, 4557–4565.
44 T. M. Nolte, W. J. G. M. Peijnenburg, A. J. Hendriks, *et al.*, *Chemosphere*, 2017, **179**, 49–56.
45 L. Guo, W. Yuan, Z. Lu, *et al.*, *Colloids Surf., A*, 2013, **439**, 69–83.
46 X. Yao, Y. Zhang, J. Lv, *et al.*, *Chemistry*, 2016, **6**, 496–501.
47 A. Othmani, R. Bunet, J.-L. Bonnefont, *et al.*, *J. Appl. Phycol.*, 2015, **3**, 1975–1986.
48 H. Shi, S. Yu, D. Liu, *et al.*, *Mar. Drugs*, 2012, **12**, 1331–1344.
49 ASTM, *Standard Practice for Evaluating Biofouling Resistance and Physical Performance of Marine Coating Systems*, vol. D 6990-2005, 2011.